Special Issue "Plant-Microbe Interactions"

Self-interaction of *Tomato spotted wilt virus* NSs protein enhances gene silencing suppressor activity, but is dispensable as avirulence determinant on pepper

A. ALMÁSI[1,*] (ID), K. NEMES[2], R. SÁRAY[1], Á. GELLÉRT[3], N. INCZE[4], P. VÁGI[5], E. BADICS[4], V. SOÓS[4], and K. SALÁNKI[1]

[1]*Plant Protection Institute, Centre for Agricultural Research, Eötvös Loránd Research Network, H-1022 Budapest, Hungary*
[2]*European Union Reference Laboratory for Foodborne Viruses, Swedish Food Agency, SE-75237 Uppsala, Sweden*
[3]*Institute for Veterinary Medical Research, Eötvös Loránd Research Network, H-1143 Budapest, Hungary*
[4]*Agricultural Institute, Centre for Agricultural Research, Eötvös Loránd Research Network, H-2462 Martonvásár, Hungary*
[5]*Institute of Experimental Medicine, Eötvös Loránd Research Network, H-1083 Budapest, Hungary*

[*]Corresponding author: E-mail: almasi.aszteria@atk.hu

Abstract

Tomato spotted wilt virus (TSWV) has significant economic impact on horticulture worldwide. One of the five proteins encoded by TSWV genome is the multifunctional NSs protein, which is a viral suppressor of RNA silencing (VSR) besides functioning as the effector of *Tsw* resistance gene in resistant pepper cultivars. In this study we demonstrate the *in vivo* self-interaction of NSs protein using bimolecular fluorescence complementation and yeast two-hybrid assays, and propose that a highly charged alpha helix located at the second half of the protein is required for self-interaction. Furthermore, we confirmed that self-interaction is not required for its effector function on pepper. Moreover, self-interaction is dispensable for gene silencing suppressor activity, although it enhances the suppression efficiency.

Keywords: avirulence determinant, hypersensitive reaction, NSs protein, self-interaction, *Tomato spotted wilt virus*, viral suppressor of RNA silencing.

Introduction

The order *Bunyavirales* is a unique group among viruses; since most of the members infect animals, and only a few representatives are plant viruses, such as *Tomato spotted wilt virus* (TSWV). TSWV is the type member of the genus *Orthotospovirus* in the family *Tospoviridae* (Abudurexiti *et al.* 2019). It was recorded as one of the most important viruses in molecular plant pathology (Parrella *et al.* 2003),

with an extremely wide host range infecting more than 1 300 plant species (Scholthof *et al.* 2011). Natural hosts of TSWV include several horticultural species like pepper, tomato, tobacco, onion, and peanut. TSWV is transmitted by thrips in circulative-propagative manner, replicating not only in the plant hosts, but also in the thrips vectors. As a remarkable plant pathogen, the geographical distribution and economic impact have increased considerably recently (Pappu *et al.* 2009, Oliver and Whitfield 2016).

The tripartite TSWV genome is built up of three single stranded RNA segments. The largest one (L RNA) has negative polarity and encodes the RNA-dependent RNA polymerase while the ambisense M and S RNAs both encode two genes each in ambisense arrangement. The membrane glycoprotein and the NSm movement protein are encoded in the M RNA, while the S RNA harbors open reading frames of the nucleocapsid protein (N) and the NSs protein. The NSs protein is multifunctional, serving as a viral suppressor of RNA silencing (VSR) (Takeda *et al.* 2002, de Ronde *et al.* 2014), with ATPase and 5' phosphatase activities, and was demonstrated to function as an avirulence factor (Avr) on pepper playing role in *Tsw* gene recognition (Margaria *et al.* 2007, de Ronde *et al.* 2013). It was shown to have RNA binding affinity to long, small dsRNAs and microRNAs (Schnettler *et al.* 2010). The NSs protein was proved essential for persistent infection and transmission by thrips (Margaria *et al.* 2014) and suppressing the jasmonate-mediated plant immunity against thrips (Wu *et al.* 2019). *Via* binding ability to multiple host proteins, NSs plays a role in TSWV-host interactions and triggers host responses as defense signaling, protein nuclear transportation, antioxidation, and stress tolerance (Zhai *et al.* 2021). The self-interaction of the NSs protein was reported in the case of another orthotospovirus, namely *Capsicum chlorosis virus* (Widana Gamage *et al.* 2017), but not in the case of TSWV. However, the complex function of NSs as a VSR and effector in pepper virus-host interaction in connection with structural features requires further characterization.

The aim of present study was to demonstrate the self-interaction of the TSWV NSs protein and to determine a highly charged alpha helix located at the second half of the protein that is required for self-interaction. The impact of dimer formation on the basic functions of the NSs protein was also verified. The experiments demonstrated that dimer formation is not required for TSWV NSs avirulence function on pepper and is dispensable for gene silencing suppressor activity, although it enhances the suppression efficiency.

Materials and methods

Plants and cultivation: Wild type and transgenic (line 16c) *Nicotiana benthamiana* Domin plants (de Ronde *et al.* 2019) were kept in a growth chamber with a 16-h photoperiod, an irradiance of 300 µmol m^{-2} s^{-1}, day/night temperatures of 23/18°C, and a relative humidity of 70%. TSWV susceptible and resistant pepper cultivars, *Capsicum annuum* L. cvs. Galga and Brody (containing the *Tsw* resistance gene) were maintained in a growth chamber at a 16-h photoperiod, an irradiance of 300 µmol m^{-2} s^{-1}, day/night temperatures of 24/21°C, and a relative humidity of 70%.

Structural bioinformatics and electrostatic analysis: The full length HUP4-2012-WT TSWV NSs protein structure model was generated with *I-TASSER* (https://zhanglab.ccmb.med.umich.edu/I-TASSER). The surface accessible, highly charged alpha helix from amino acids (aa) 336 to 356 was cut out from the whole model using the academic version of the *Schrödinger Maestro* (https://www.schrodinger.com/freemaestro). The mutant (NSs/R337A, NSs/H340A, and NSs/E344A) alpha helices were created with the mutate residue option of the *Schrödinger Maestro*. Cartoon style molecular graphics were created with *PyMOL 1.8.0.3* molecular graphic system (https://pymol.org/2) (DeLano 2016). Electrostatic potential maps were calculated with *Adaptive Poisson-Boltzmann Solver* (APBS) *v. 1.3* (Baker *et al.* 2001) using the linearized Poisson-Boltzmann method (Gilson *et al.* 1988) with a dielectric constant of 78.0 and 2 for the water solvent and protein core, respectively. The partial charges for the electrostatic potential calculations were calculated with *PDB2PQR* (Dolinsky *et al.* 2004).

Plasmid constructs: *NSs* gene of the HUP4-2012-WT TSWV isolate used in this study was cloned previously (Almási *et al.* 2015). Mutant NSs proteins (NSs/R337A, NSs/H340A, and NSs/E344A) were generated by site-directed mutagenesis with overlap PCR using the oligonucleotides TSWV NSs SacI for and TSWV NSs BamHI rev (for oligonucleotide sequences *see* Table 1 Suppl.) and cloned into *pGEM®-T Easy* plasmid vector (*Promega*, Madison, WI, USA), before being subcloned into pBIN61s binary vector enclosing 35S promoter and NOS terminator (Silhavy *et al.* 2002). For the bimolecular fluorescence complementation (BiFC) assay, the N- and C-terminal fragments of yellow fluorescent protein (YFP) were fused to the C-terminus of the NSs protein and the mutant clones using the TSWV-NSs-BiFC forward and reverse primers (Table 1 Suppl.), and were cloned into vectors Gateway™ pDONR™221 and pGWBc-nYFP, and pGWBc-cYFP (pNSs-YFP^N and pNSs-YFP^C) utilizing the *GATEWAY* technology (*Invitrogen*, Waltham, MA, USA) (Nakagawa *et al.* 2007).

Agroinfiltration: BiFC assay and *Agrobacterium*-mediated transient expression in *N. benthamiana* leaves were conducted by pressure infiltration as described previously (Almási *et al.* 2015). The constructs of *A. tumefaciens* were infiltrated in 4- to 6-week-old *N. benthamiana* leaves *via* agroinfiltration (absorbance A_{600} was adjusted to 0.5).

In the RNA silencing suppression (RSS) activity experiment, A_{600} of the constructs was adjusted to 0.2 and A_{600} of the *Agrobacterium* culture of green fluorescent protein (GFP)-expressing strain was adjusted to 0.4 (Nemes *et al.* 2014). Four days after inoculation (dai) the GFP fluorescence was detected using *iBright FL1500* imaging system (*Thermo Fisher Scientific*, Waltham, Massachusetts, USA).

For the HR induction assay, the same *A. tumefaciens* constructs were used as in the RSS assay and agroinfiltration of *C. annuum* cv. Brody or cv. Galga leaves was performed with A_{600} adjusted to 0.5. The formation or lack of HR was assessed at 5 dai.

Live cell imaging: Leaves (3 dai) were stained with 1 mM 4′,6-diamidino-2-phenylindole (DAPI) and analyzed by *Nikon Ti* (*Nikon*, Tokyo, Japan) inverted microscope equipped with *A1plus* confocal scan head. The images were obtained with *Nikon Plan Apo VC 20x DIC N2* objective, 405 nm excitation/450 nm emission for DAPI channel, 488 nm excitation/525 nm emission for YFP signal, transmitted detector for the transmitted light channel. Imaging parameters were controlled by a *NIKON NIS-Elements AR* software.

Electrolyte leakage experiment: Electrolyte leakage experiment was carried out with TSWV resistant pepper plants (*C. annuum* cv. Brody) agroinfiltrated with the same constructs as in the HR induction assay. Leaf disks (4 - 5) were cut out from the infiltrated leaf area (0.9 cm in diameter) three dai after infiltration, fresh mass was measured and then discs were floated on distilled water (15 cm³) surface for 4 h. Electric conductivity of the bathing solutions was measured by a conductivity bridge (*Oakton Benchtop Meter*, *type pH/Con 510*, *Oakton/Eutech Instruments Pte Ltd.*, Singapore) as described by Ádám *et al.* (2000) formerly.

Yeast two-hybrid assay: The self-interaction of TSWV NSs was carried out according to the manufacturer's protocol (*Matchmaker Gold* yeast two-hybrid system, *Takara Bio*, Mountain View, California, USA). Wild type NSs and the mutants (NSs/R337A, NSs/H340A, and NSs/E344A) were either bait (N-terminal GAL4 DNA binding domain fusions), or prey (N-terminal GAL4 activation domain fusions). The p53 + T cell antigen interaction was a positive, T cell antigen + lamin interaction was used as a negative control. Empty pGBKCg vector was used as a negative autoactivation control for NSs - BD domain interactions. The pGBKCg-NSs and pGADCg-NSs constructs were co-transformed into yeast strain Y2HGold. Yeast co-transformed with the indicated plasmids was spotted onto synthetic medium (SD/-Ade/-His/-Leu/-Trp) containing 10 mM 3-amino-1,2,4-triazole and 0.04 mg cm⁻³ X-α-gal. The empty vectors pGBKCg (BD) and pGADCg (AD) were used as negative controls.

Quantitative real-time PCR assays: Fresh *N. benthamiana* leaf tissue was ground in liquid N_2 and extracted with *SV Total* RNA isolation system (*Promega*, Madison WI). RNA concentration was measured with *Nanodrop* spectrophotometer (*Thermo Fisher Scientific*, Waltham, MA, USA). Reverse transcription (RT) reaction was performed with *RevertAid First Strand* cDNA synthesis kit (*Fermentas*, Waltham, MA, USA) according to the manufacturer's instructions. All samples were run in triplicates. Forward and reverse primers (GFP real-time for and GFP real-time rev) used for GFP mRNA analysis are available in Table 1 Suppl. For the detection of nY-ends of the BiFC constructs, forward and reverse primers (BiFC real-time for and BiFC real-time rev, Table 1 Suppl.) were used and *N. benthamiana* elongation factor-1 alpha (*EF1α*) mRNA (GenBank accession number CN744397.1) served as an internal control (amplified with oligonucleotides EF1α for and rev, *see* in Table 1 Suppl.). Real-time PCR was carried out in a *BioRad CFX96 TouchTM* machine (*BioRad*, Hercules, CA, USA) with a thermal cycling profile described previously (Nemes *et al.* 2014).

Western blot analysis was carried out as described formerly (Nemes *et al.* 2014, 2017). Protein samples were extracted from *N. benthamiana* leaf discs (fresh mass of 20 mg) and were separated on 8% (m/v) SDS-PAGE gels. The equal amount of the loading was verified by Coomassie staining. Proteins were transferred to *Hybond-C* membrane (*GE Healthcare*, Buckinghamshire, UK) and subjected to immunoblot analysis with rabbit anti-N-YFP (1:2 000) or anti-GFP primary antibodies (1:3 000) (*Agrisera*, Vännäs, Sweden), respectively, and HRP-conjugated (1:5 000) or AP-conjugated (1:2 500) anti-rabbit IgG (*BioRad*) as secondary antibodies, respectively. The AP-conjugated anti-rabbit IgG was detected with BCIP/NBT substrate, while anti-N-YFP/HRP-conjugated anti-rabbit IgG was detected with chemiluminescent substrate/reagent (*Pierce ECL* Western blotting substrate, *Thermo Fisher Scientific*) by *iBright Imaging* system.

Statistical analysis: Regarding the statistical analysis of the electrolyte leakage assay and the RSS activity assays, data were analyzed by Kolmogorov-Smirnov test for normality of the data, and Levene's test for homogeneity of variances. To evaluate the differences between the areas of the induced local necrotic lesions one-way *ANOVA* model coupled with Games-Howell's post hoc test were used. The statistical analysis was carried out using *IBM SPSS Statistics 25* and *MS Excel*. Descriptive statistics and statistical analysis are detailed in Fig. 1 Suppl.

Results

First, the potential self-interaction of just the wild type (WT) TSWV NSs protein was evaluated with BiFC using the previously described and cloned *NSs* gene of the HUP4-2012-WT isolate (Almási *et al.* 2015). The N-terminal (YFP^N), and C-terminal (YFP^C) fragments of YFP were fused to the C-terminus of the NSs protein, respectively, to generate the constructs pNSs-YFP^N and pNSs-YFP^C. *Agrobacterium*-mediated transient expression in *N. benthamiana* leaves was conducted by pressure infiltration as described previously (Nemes *et al.* 2017, 2019). The fluorescent signals were detected *via* confocal microscopy 3 dai. Strong YFP fluorescence was observed in the cytoplasm only in the case of co-infiltration of the pNSs-YFP^N and pNSs-YFP^C, demonstrating self-interaction of TSWV NSs protein (Fig. 1*A*). Furthermore, yeast two-hybrid (Y2H) assay also confirmed the self-interaction of the WT NSs protein (Fig. 1*D*).

A conserved alpha helix located between aa 335 - 356 in the TSWV NSs protein was previously identified to play a role in the loss of hypersensitive reaction (HR)
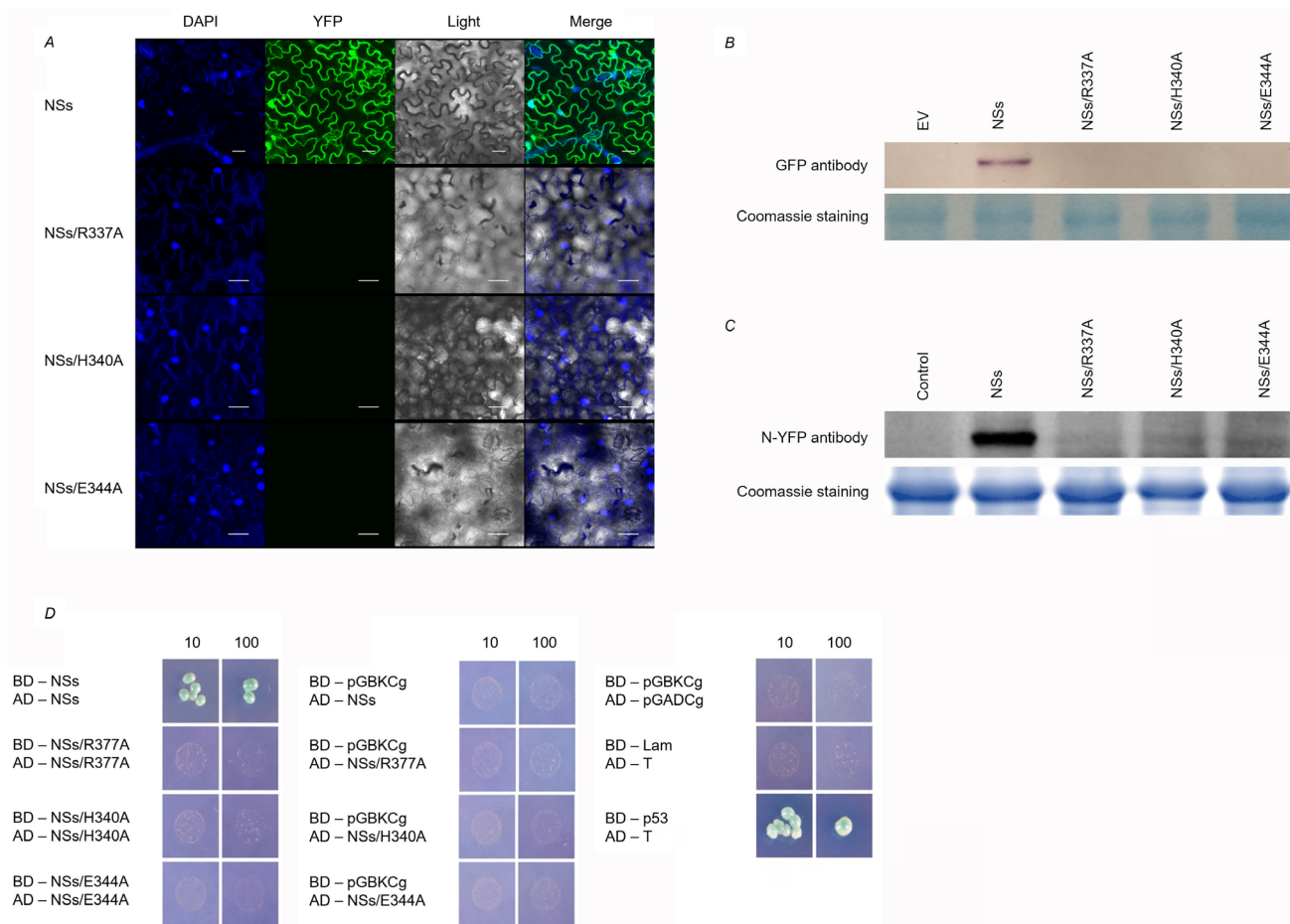
Fig. 1. Self-interaction of TSWV NSs protein demonstrated by bimolecular fluorescence complementation (BiFC) and by yeast two-hybrid assays (Y2H). *A* - Images recorded by confocal laser microscopy 3 d after agroinfiltration. *Scale bar*: 20 μm. From left to right: the DAPI, YFP fluorescence spectrum, bright field, and overlay signals. *B* - Western blot detection of the NSs-YFP protein in the BiFC assay using anti-GFP polyclonal antibody. *C* - Western blot analysis of BiFC assay co-infiltrated with NSs using anti-N-YFP antibody. *D* - Self-interaction of the NSs protein and the mutants (NSs/R337A, NSs/H340A, and NSs/E344A) in a Y2H system.

induction and RSS activity (de Ronde *et al*. 2014). In the present study structural characterization of this alpha helix was carried out. The modeling of the three-dimensional structure of this alpha helix facilitated the identification of a highly charged surface region at the terminal section of the helix. This region is formed by amino acids R337, H340, and E344, which is located on the putative outer surface of the NSs protein acting as potential hot spots for protein interaction (Fig. 2*A,B*). Mutation of these charged amino acids to hydrophobic alanine induce significant electrostatic surface potential changes demonstrated on Fig. 2*B,D,F,H*.

To assess the function of the alpha helix, the previously identified charged amino acids were replaced with a neutral alanine by site directed mutagenesis resulting in three mutants, namely NSs/R337A, NSs/H340A, and NSs/E344A. The mutations were introduced to the NSs by overlap PCR followed by cloning to test their self-interaction by BiFC and Y2H assays. At 3 dai none of the mutant BiFC constructs emitted fluorescence in contrast

to the WT NSs on *N. benthamiana* leaves (Fig. 1*A*). The stability of the WT and the mutant NSs proteins were evaluated with Western blot analysis. Since NSs antibody is not available, GFP polyclonal antibody or N-YFP antibody were used to detect the proteins bearing the N-terminal fragments of YFP fused to the C-terminus of the NSs protein (NSs-YFP[N]). At 3 dai the WT NSs-YFP[N] was detected, but the NSs/R337A-YFP[N], NSs/H340A-YFP[N], and NSs/E344A-YFP[N] mutants were not detectable (Fig 1*B*). If NSs of the TSWV WT strain as an efficient suppressor of gene silencing without the YFP[N] fusion was co-infiltrated with the NSs/R337A-YFP[N], NSs/H340A-YFP[N], and NSs/E344A-YFP[N] constructs, the mutant fusion proteins were detectable with the N-YFP antibody (Fig. 1*C*) even if in significantly smaller quantities then in the WT NSs-YFP[N]. In Y2H experiment, a strong affinity of wild type NSs for self-interaction was observed, but all of the NSs mutations (NSs/R337A, NSs/H340A, and NSs/E344A) abolished growth on selective media indicating that these aa residues are essential for self-
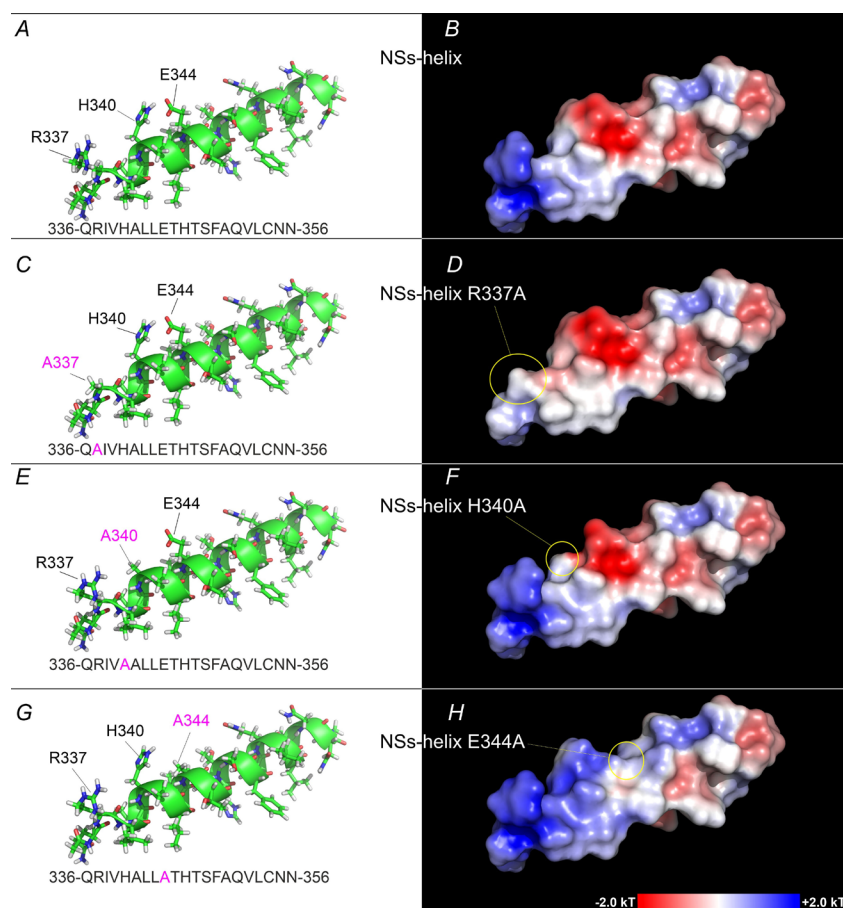
Fig. 2. Putative surface helix from the TSWV NSs protein. Cartoon representations show the three-dimensional structures of the wild-type TSWV NSs alpha helix (*A*) and its mutated versions (*C*, *E*, and *G*). Electrostatic surface views of these helices are presented on the right panel (*B*, *D*, *F*, and *H*). *Red* represents regions with potential value less than -2.0 kT; *white* represents 0.0; *blue* shows regions greater than +2.0 kT. Regions around the mutated positions are encircled in order to easily recognize the electrostatic changes. Cartoon style molecular graphics (*A*, *C*, *E*, and *G*) were created with *PyMOL*.

interaction (Fig. 1*D*). The results of the BiFC and Y2H assays consistently demonstrated that the three mutations could hamper the NSs protein self-interaction independently.

The effect of these amino acid alterations was further analyzed on the primary functions of NSs such as effector of HR (Avr) and RSS activity. *Tsw* gene effector function of the NSs protein was analyzed by its ability to elicit HR on *C. annuum*. A binary vector expressing WT and mutant NSs proteins (NSs/R337A, NSs/H340A, and NSs/E344A) were agroinfiltrated into leaves of TSWV susceptible and resistant pepper cultivars, *C. annuum* cv. Galga and cv. Brody (containing the *Tsw* resistance gene), respectively, as described previously (Almási *et al.* 2017). The infiltration experiments were repeated three times. After 5 dai the WT NSs as well as the mutant constructs induced HR on the leaves of the resistant cv. Brody, while necrosis was not detected on the susceptible cv. Galga (Fig. 3*A*). This result indicates that self-interaction is not required for the *Tsw* effector function of NSs.

To evaluate the hypersensitive response in the infiltrated leaves, the rates of ion leakage were studied. The infiltration of NSs, NSs/R337A, NSs/H340A, and NSs/E344A had significant effect on ion leakage, the electric conductivity clearly increased in the case of all the constructs compared to the p14 control infiltration. Significant variation of the electric conductivity was not detected among the WT and the different mutant constructs (Fig. 3*B*).

Since the main function of the NSs protein is the gene silencing suppression, the RSS activity of the WT and mutant NSs proteins was analyzed. In the agroinfiltration assay, a binary vector expressing the WT NSs and the mutant constructs were co-infiltrated with GFP reporter gene in *N. benthamiana* 16c plants (silenced for GFP expression). The suppressor activities were monitored by visual observation of the GFP fluorescence, and the quantification of the RSS activity was evaluated by measuring the mRNA accumulation of GFP mRNA in the infiltrated patches by RT-qPCR at 6 dai (Fig. 4*A*). The RSS activity was reduced in the case of all mutants according to the visual observation (Fig. 4*A*). The RT-qPCR analysis supported the visual observation and significant
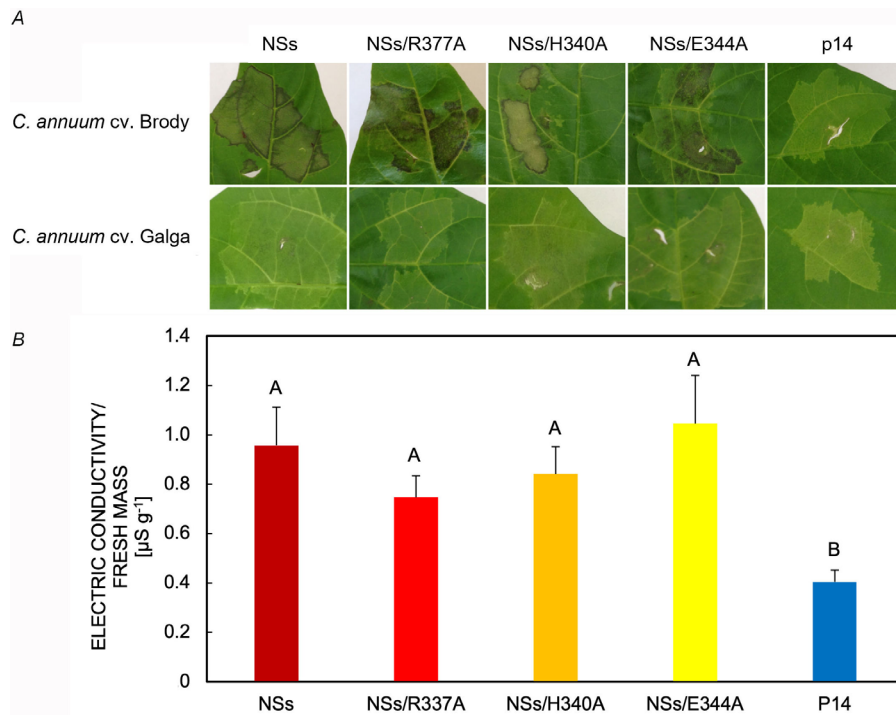
Fig. 3. *A* - HR induction assay of TSWV NSs Avr factor on *C. annuum* cv. Brody harboring the *Tsw* resistance gene (*top panel*) or *C. annuum* cv. Galga, susceptible to TSWV (*bottom panel*) by transient expression. P14-containing (a tombusvirus VSR) construct served as negative control. *B* - Electrolyte leakage experiment with the agroinfiltrated resistant pepper plants with the NSs construct of the WT TSWV, NSs/R337A, NSs/H340A, and NSs/E344A. P14 was used as negative control.
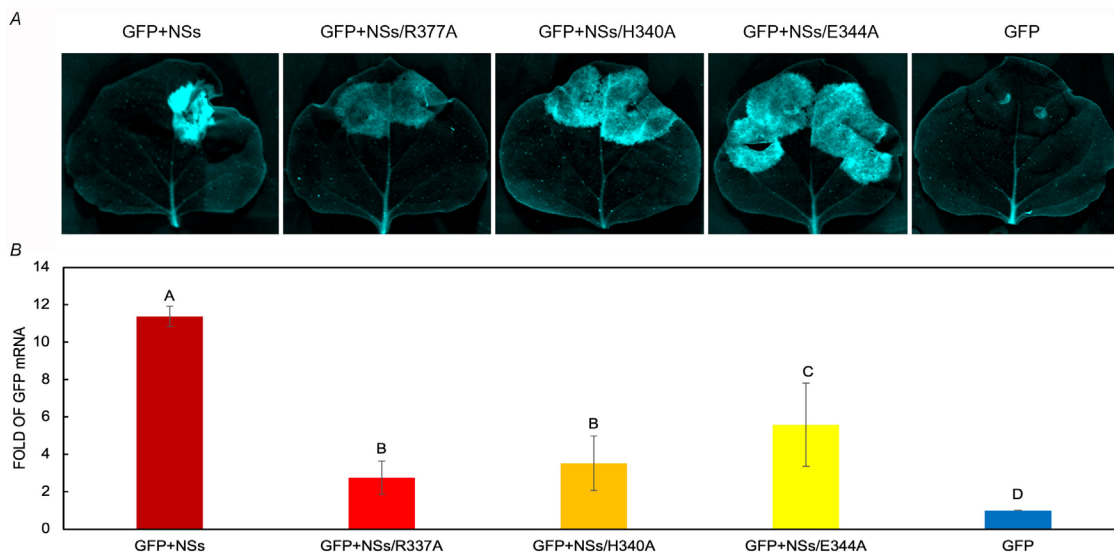

Fig. 4. *A* - Suppression of RNA silencing in patch assays. Binary vectors expressing WT and mutant NSs proteins were co-infiltrated with binary vector expressing GFP into *N. benthamiana* 16c leaves (GFP+NSs, GFP+NSs/R377A, GFP+NSs/H340A, GFP+NSs/E344A). Binary vector expressing GFP alone served as negative control (GFP). *B* - The diagram shows the accumulation of GFP mRNA in agroinfiltrated patches measured by RT-qPCR.

reduction was found between the mRNA GFP content in the infiltrated patches of the WT and the NSs mutants ($P < 0.0001$) (Fig. 4*B*). These results indicate that self-interaction of NSs enhances its RSS activity, although dispensable for this function.

Discussion

The self-interaction is a general feature of the viral suppressor proteins, and the oligomer structure determines the RNA binding capacity of the protein (Foss *et al.* 2019). Although the structural characterization of several viral suppressor proteins (*e.g.*, tomato aspermy virus 2b protein, cymbidium ringspot virus p19) were accomplished based on crystallization data and the functional requirement was evaluated in detail (Vargason *et al.* 2003, Chen *et al.* 2008), the structure of TSWV NSs protein is still unknown. Different TSWV NSs protein structures were generated by state-of-the-art protein structure prediction methods and the resulted models were completely distinct from each other (Olaya *et al.* 2019), however, the evaluation of shorter segments of the protein is feasible. In the present study, a conserved alpha helix located between aa 335 - 356 of TSWV NSs protein was analyzed. Primarily, the three-dimensional structure of this alpha helix was predicted, and a highly charged surface region was identified (R337, H340, and E344) as a potential hot spot for protein interaction (Fig. 2). Charged alpha helices were identified as important motifs in protein-protein interactions (Azzarito *et al.* 2013). The self-interaction of the TSWV NSs protein was demonstrated and the role of the highly charged region in self-interaction was confirmed (Fig. 1). This alpha helix was assayed previously using point mutations (N355A/N356A) and resulted in loss of HR induction and RSS activity (de Ronde *et al.* 2014). The deletion of the homologous conserved region of the watermelon silver mottle virus NSs protein (aa 333 - 375) caused loss of RSS function and the truncated protein accumulation was undetectable (Huang *et al.* 2015), similarly to the NSs/R337A, NSs/H340A, and NSs/E344A mutants described in the present study, where protein accumulation could only be detected in the presence of an entirely functional WT NSs (*via* co-infiltration) (Fig. 1). The self-interaction of an orthotospovirus, the *Capsicum chlorosis virus* NSs protein was demonstrated recently (Widana Gamage *et al.* 2017), although the involvement of self-interaction in RSS activity was not verified. Here, we demonstrated that self-interaction of TSWV NSs protein is not essential for RSS activity; however, the self-interaction enhanced the RSS efficiency. The mutant NSs proteins accumulated to a lower amount than WT NSs which also could have contribution to the reduced RSS activity. The GW/WG motif of TSWV NSs protein (at aa position 17/18) was reported to be involved in the interaction with *ARGONAUTE 1* (AGO1) (Giner *et al.* 2010), and the mutation of this region proved that this motif is crucial for both RSS and effector activity (de Ronde *et al.* 2014), suggesting a putative interaction with AGO1. The interaction of the NSs and AGO1 proteins was further proposed by Hedil *et al.* (2015), NSs mutants W17A/G18A were hampered in local RSS activity but they still were able to suppress GFP silencing in systemic leaves. These results suggested that residues W17/G18 act by another way downstream of siRNA biogenesis and sequestration.

In the lack of NSs self-interactions, the monomer is still able to inhibit the antiviral activity of the host RNA-induced silencing complex through direct interaction with AGO1 or with other components of the gene silencing complex in monomeric form. Currently several VSRs are considered to be multifunctional (Fang and Qi 2016, Widana Gamage *et al.* 2017, Valli *et al.* 2018), so they can presumably interact with different steps of the RNA silencing pathway. For example, the cucumber mosaic virus 2b interaction with AGO1 proved to be crucial for the suppression of RDR-dependent antiviral silencing while the other function, the RNA binding, seems to be dispensable (Fang and Qi 2016) and can contribute to the fine-tuning of the RSS.

For pepper breeders only the *Tsw* gene originated from *Capsicum chinense* is available that confers resistance to TSWV (Boiteux and de Ávila 1994). The *Tsw*-governed resistance is induced by the NSs protein of TSWV (Margaria *et al.* 2007, de Ronde *et al.* 2013) and the N terminal part seems to be fundamental for HR triggering according to the analysis of a series of mutants (Margaria *et al.* 2007). The *Tsw* gene was cloned recently and identified as a nucleotide-binding leucine-rich repeat (NLR) protein (Kim *et al.* 2017, van Grinsven *et al.* 2022) with a coiled-coil (CC) domain, a nucleotide-binding domain, and eight leucine-rich repeats (LRR). The LRR domain is generally associated with the recognition of an effector. In this case, the effector is the NSs protein, even if direct interaction was not proved experimentally so far. According to our results, even if the NSs protein can establish self-interaction, the monomer form is sufficient to elicit HR (Fig. 3). Remarkably, in the resistance breaking (RB) NSs mutants derived from different geographical regions no consensus mutations are present (Margaria *et al.* 2007, de Ronde *et al.* 2013, 2019; Almási *et al.* 2015, 2020; Ferrand *et al.* 2015, Jiang *et al.* 2017). Up to now, experimentally one single-point mutation at amino acid position 104 was identified to be responsible for the resistance breaking phenotype of the NSs protein (Almási *et al.* 2017). Since the RB phenotype was obviously developed by several distinct mutations, the complex structural-functional characterization of the interaction network between the resistance gene and the viral effector could contribute to the understanding of the complete mechanism.

References

Abudurexiti A., Adkins S., Alioto D. *et al.*: Taxonomy of the order *Bunyavirales*: update 2019. - Arch. Virol. **164**: 1949-1965, 2019.

Ádám A.L., Galal A.A., Manninger K., Barna B.: Inhibition of the development of leaf rust (*Puccinia recondita*) by treatment of wheat with allopurinol and production of a hypersensitive-like reaction in a compatible host. - Plant Pathol. **49**: 317-323, 2000.

Almási A., Csilléry G., Csömör Z. *et al.*: Phylogenetic analysis of *Tomato spotted wilt virus* (TSWV) NSs protein demonstrates the isolated emergence of resistance-breaking strains in

pepper. - Virus Genes **50**: 71-78, 2015.

Almási A., Nemes K., Csömör Z. *et al.*: A single point mutation in *Tomato spotted wilt virus* NSs protein is sufficient to overcome *Tsw*-gene-mediated resistance in pepper. - J. Gen. Virol. **98**: 1521-1525, 2017.

Almási A., Nemes K., Salánki K.: Increasing diversity of resistance breaking pepper strains of *Tomato spotted wilt virus* in the Mediterranean region. - Phytopathol. Mediterr. **59**: 385-391, 2020.

Azzarito V., Long K., Murphy N.S., Wilson A.J.: Inhibition of α-helix-mediated protein–protein interactions using designed molecules. - Nature Chem. **5**: 161-173, 2013.

Baker N.A., Sept D., Joseph S. *et al.*: Electrostatics of nanosystems: Application to microtubules and the ribosome. - P. Natl. Acad. Sci. USA **98**: 10037-10041, 2001.

Boiteux L.S., de Ávila A.C.: Inheritance of a resistance specific to tomato spotted wilt *tospovirus* in *Capsicum chinense* 'PI159236.' - Euphytica **75**: 139-142, 1994.

Chen H., Yang J., Lin C., Yuan Y.A.: Structural basis for RNA-silencing suppression by *Tomato aspermy virus* protein 2b. - EMBO Rep. **9**: 754-760, 2008.

de Ronde D., Butterbach P., Lohuis D. *et al.*: *Tsw* gene-based resistance is triggered by a functional RNA silencing suppressor protein of the *Tomato spotted wilt virus*. - Mol. Plant Pathol. **14**: 405-415, 2013.

de Ronde D., Lohuis D., Kormelink R.: Identification and characterization of a new class of *Tomato spotted wilt virus* isolates that break *Tsw*-based resistance in a temperature-dependent manner. - Plant Pathol. **68**: 60-71, 2019.

de Ronde D., Pasquier A., Ying S. *et al.*: Analysis of *Tomato spotted wilt virus* NSs protein indicates the importance of the N-terminal domain for avirulence and RNA silencing suppression. - Mol. Plant Pathol. **15**: 185-195, 2014.

DeLano W.L.: The PyMOL Molecular Graphics System, version 1.8., Schrödinger LLC, 2016.

Dolinsky T.J., Nielsen J.E., McCammon J.A., Baker N.A.: PDB2PQR: An automated pipeline for the setup of Poisson-Boltzmann electrostatics calculations. - Nucleic Acids Res. **32**: W665-W667, 2004.

Fang X., Qi Y.: RNAi in plants: An Argonaute-centered view. - Plant Cell **28**: 272-285, 2016.

Ferrand L., García M.L., Resende R.O. *et al.*: First report of a resistance-breaking isolate of *Tomato spotted wilt virus* infecting sweet pepper harboring the *Tsw* gene in Argentina. - Disease Notes **99**: 1869, 2015.

Foss D.V., Schirle N.T., MacRae I.J., Pezacki J.P.: Structural insights into interactions between viral suppressor of RNA silencing protein P19 mutants and small RNAs. - FEBS Openbio **9**: 1042-1051, 2019.

Gilson M.K., Sharp K.A., Honig B.H.: Calculating the electrostatic potential of molecules in solution: Method and error assessment. - J. Comput. Chem. **9**: 327-335, 1988.

Giner A., Lakatos L., García-Chapa M. *et al.*: Viral protein inhibits RISC activity by Argonaute binding through conserved WG/GW motifs. - PLoS Pathog. **6**: e1000996, 2010.

Hedil M., Sterken M.G., de Ronde D. *et al.*: Analysis of tospovirus NSs proteins in suppression of systemic silencing. - PLoS ONE **10**: e0134517, 2015.

Huang C.-H., Hsiao W.-R., Huang C.-W. *et al.*: Two novel motifs of *Watermelon silver mottle virus* NSs protein are responsible for RNA silencing suppression and pathogenicity. - PLoS ONE **10**: e0126161, 2015.

IJiang L., Huang Y., Sun L. *et al.*: Occurrence and diversity of *Tomato spotted wilt virus* isolates breaking the *Tsw* resistance gene of *Capsicum chinense* in Yunnan, southwest China. -

Plant Pathol. **66**: 980-989, 2017.

Kim S.-B., Kang W.-H., Huy H.N. *et al.*: Divergent evolution of multiple virus-resistance genes from a progenitor in *Capsicum* spp. - New Phytol. **213**: 886-899, 2017.

Margaria P., Bosco L., Vallino M. *et al.*: The NSs protein of *Tomato spotted wilt virus* is required for persistent infection and transmission by *Frankliniella occidentalis*. - J. Virol. **88**: 5788-5802, 2014.

Margaria P., Ciuffo M., Pacifico D., Turina M.: Evidence that the nonstructural protein of *Tomato spotted wilt virus* is the avirulence determinant in the interaction with resistant pepper carrying the *Tsw* gene. - Mol. Plant Microbe. Interact. **20**: 547-558, 2007.

Nakagawa T., Suzuki T., Murata S. *et al.*: Improved Gateway binary vectors: High-performance vectors for creation of fusion constructs in transgenic analysis of plants. - Biosci. Biotech. Bioch. **71**: 2095-2100, 2007.

Nemes K., Gellért Á., Almási A. *et al.*: Phosphorylation regulates the subcellular localization of *Cucumber mosaic virus* 2b protein. - Sci. Rep.-UK **7**: 13444, 2017.

Nemes K., Gellért Á., Balázs E., Salánki K.: Alanine scanning of *Cucumber mosaic virus* (CMV) 2b protein identifies different positions for cell-to-cell movement and gene silencing suppressor activity. - PLoS ONE **9**: e112095, 2014.

Nemes K., Gellért Á., Bóka K. *et al.*: Symptom recovery is affected by *Cucumber mosaic virus* coat protein phosphorylation. - Virology **536**: 68-77, 2019.

Olaya C., Adhikari B., Raikhy G. *et al.*: Identification and localization of *Tospovirus* genus-wide conserved residues in 3D models of the nucleocapsid and the silencing suppressor proteins. - Virol. J. **16**: 7, 2019.

Oliver J.E., Whitfield A.E.: The genus *Tospovirus*: Emerging bunyaviruses that threaten food security. - Annu. Rev. Virol. **3**: 101-124, 2016.

Pappu H.R., Jones R.A.C., Jain R.K.: Global status of tospovirus epidemics in diverse cropping systems: Successes achieved and challenges ahead. - Virus Res. **141**: 219-236, 2009.

Parrella G., Gognalons P., Gebre-Selassie K. *et al.*: An update of the host range of *Tomato spotted wilt virus*. - J. Plant Pathol. **85**: 227-264, 2003.

Schnettler E., Hemmes H., Huismann R. *et al.*: Diverging affinity of tospovirus RNA silencing suppressor proteins, NSs, for various RNA duplex molecules. - J. Virol. **84**: 11542-11554, 2010.

Scholthof K.-B.G., Adkins S., Czosnek H. *et al.*: Top 10 plant viruses in molecular plant pathology. - Mol. Plant Pathol. **12**: 938-954, 2011.

Silhavy D., Molnár A., Lucioli A. *et al.*: A viral protein suppresses RNA silencing and binds silencing-generated, 21- to 25-nucleotide double-stranded RNAs. - EMBO J. **21**: 3070-3080, 2002.

Takeda A., Sugiyama K., Nagano H. *et al.*: Identification of a novel RNA silencing suppressor, NSs protein of *Tomato spotted wilt virus*. - FEBS Lett. **532**: 75-79, 2002.

Valli A.A., Gallo A., Rodamilans B. *et al.*: The HCPro from the *Potyviridae* family: An enviable multitasking helper component that every virus would like to have. - Mol. Plant Pathol. **19**: 744-763, 2018.

van Grinsven I.L., Martin E.C., Petrescu A.-J., Kormelink R.: Tsw – A case study on structure-function puzzles in plant NLRs with unusually large LRR domains. - Front. Plant Sci. **13**: 983693, 2022.

Vargason J.M., Szittya G., Burgyán J., Hall T.M.T.: Size selective recognition of siRNA by an RNA silencing suppressor. - Cell **115**: 799-811, 2003.

Widana Gamage S.M.K., Dietzgen R.G.: Intracellular localization, interactions and functions of *Capsicum chlorosis virus* proteins. - Front. Microbiol. **8**: 612, 2017.

Wu X., Xu S., Zhao P. *et al*.: The *Orthotospovirus* nonstructural protein NSs suppresses plant MYC-regulated jasmonate signaling leading to enhanced vector attraction and performance. - PLoS Pathog. **15**: e1007897, 2019.

Zhai Y., Gnanasekaran P., Pappu H.R.: Identification and characterization of plant-interacting targets of *Tomato spotted wilt virus* silencing suppressor. - Pathogens **10**: 27, 2021.